New Supercapacitors of Hybrid Configurations

Nuevos supercondensadores de configuración híbrida

Katsuhiko Naoi[1] and Wako Naoi[2]

[1]Department of Applied Chemistry, Tokyo University of Agriculture & Technology, 2-24-16 Naka-cho, Koganei, Tokyo 184-8558, Japan

[2]Division of Art and Innovative Technologies, K & W Inc, 1-3-16-901 Higashi, Kunitachi, Tokyo 186-0002, Japan.

Abstract

In recent years, the improvement of the energy density of nano-composite battery materials has been object of great study. Hybridizing battery and capacitor materials overcome the energy density limitation of existing generation-I capacitors without much sacrificing the cycling performances. Normal battery-capacitor hybrids employ high-energy & sluggish redox electrode and low-energy & fast double-layer electrodes, possibly producing a larger working voltage and higher over-all capacitance. In order to smoothly operate such asymmetric systems, however, the rates of the two different electrodes must be highly balanced. Especially, the redox rates of the battery electrodes must be substantially increased to the levels of double-layer process. In this report, we attempt to identify the essential issues for the realizable hybrids and suggest ways to overcome the rate enhancement by exemplifying ultrafast performance of the $Li_4Ti_5O_{12}$ nanocrystal prepared via a unique *in-situ* material processing technology under ultra-centrifuging.

Resumen

En los últimos años, la mejora de la densidad energética de los nanocompositos empleados en baterías ha sido objeto de un intenso estudio. La unión de un material de baterías y uno de condensadores resuelve las limitaciones de los condensadores de primera generación desde el punto de vista de la densidad energética, sin sacrificar demasiado su comportamiento frente al ciclado. Los híbridos batería-condensador usuales emplean un electrodo redox de alta energía pero lento y otro de doble capa con baja energía y rápido, que posiblemente permiten un mayor voltaje de trabajo y poseen una capacidad global más elevada. Sin embargo, para operar de forma adecuada estos sistemas asimétricos, las velocidades de estos dos electrodos deben ser compensadas. Especialmente, se deben aumentar sustancialmente las velocidades de los procesos redox del electrodo de batería hasta alcanzar las velocidades del proceso de doble capa. En el presente estudio se intentan identificar los aspectos clave para conseguir sistemas híbridos y se sugieren formas de aumentar la velocidad, mostrando como ejemplo el funcionamiento ultrarrápido de nanocristales de $Li_4Ti_5O_{12}$ preparados mediante una tecnología única in-situ aplicando ultracentrifugación.

1. Introduction

Energy storage devices are some of the most promising and important environmental technologies that are highly influential in advancing our civilization's abilities and standard of living [1-3]. Specifically, electrochemical capacitors are efficient energy storage devices that exhibit long lifespans and rapid charging and discharging [4-10]. Thus, the capacitor technology is regarded as a promising means for storing electricity [1-6]. This technology has an additional advantage of increasing effectiveness when combined with renewable (wind and solar) energy sources [6,11]. In recent years, electrochemical capacitors have been vigorously researched in hopes to improve their energy density. However, since electrochemical capacitors generally have low energy densities (below 10 Wh L^{-1}), their uses are limited and cannot fully meet performance demands required by existing electrical equipment and electronic devices. In the case of automobiles and smart grids, new energy storage devices necessitate both the attributes of lithium ion batteries, allowing high energy density, and the characteristics of electrochemical capacitors of fast charge-discharge rates in order to optimize the energy and power densities.

Such hybrid approaches can overcome the energy density limitation of the conventional electrochemical capacitors because they employ both the system of a battery-like (faradic) electrode and a capacitor-like (non-faradic) electrode, producing a larger working voltage and capacitance [6,10]. These systems can double or triple the energy density up to 20-30 Wh L^{-1} compared to that of conventional electrochemical capacitors. However, the ion exchange rates at the faradic electrodes must be increased to the levels of non-faradic electrodes in order to balance the two systems. To meet these demands, state-of-the-art nanomaterial specifically carbon nanotubes are actively applied to form composites enhancing the energy-power capability effectively [12,13]. The authors developed and applied an original *in-situ* material processing technology called 'UC treatment' to prepare an ultrafast $Li_4Ti_5O_{12}$ (LTO) electrode material (hereafter abbreviated as UC-LTO). The UC treatment relies on centrifuging, which induces simultaneous synthesis of nanoscale oxide particles *via* a sol-gel reaction and as a result hybridizes, entangles, and confines these structures into carbon matrices [14-16]. We first applied this method for the preparation of nanodot hydrous RuO_2 [14] for aqueous supercapacitors that produced a tenfold increase in capacitance (1000 F g^{-1}) over conventional activated carbon capacitor electrodes (100-140 F g^{-1}). By combining the established material selections for batteries and capacitors, the UC treatment enhances the cohesion of the two initially divergent principles into a novel hybrid concept that is capable of meeting and even exceeding the current energy and power demands.

In this paper, we focused on one of the Li^+ insertion compounds, LTO, which is a well-known Li-ion battery material. The LTO has the following advantages: 1) high columbic efficiency close to a theoretical capacity of 175 mAh g^{-1} [17-19], 2) thermodynamically flat discharge profile at 1.55 V *vs.* Li/Li^+[18,20], 3) zero-strain insertion that provides little volume change

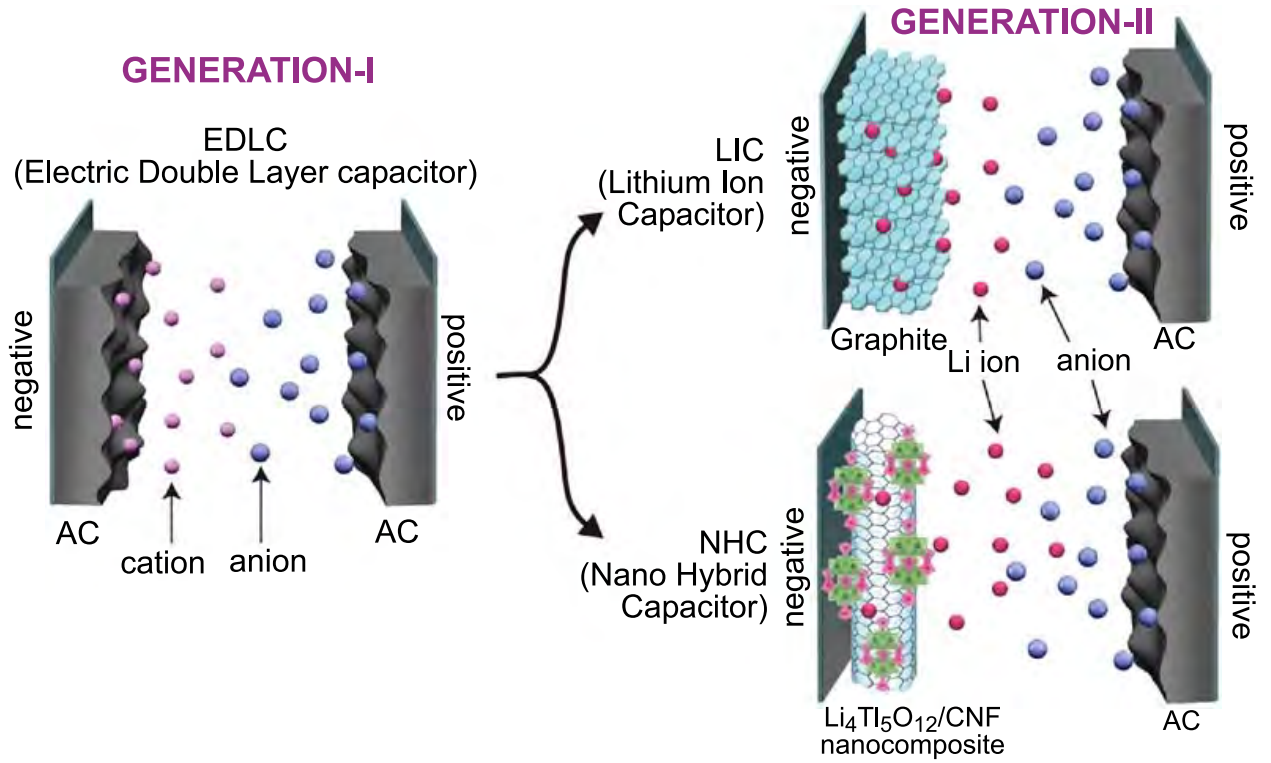

Figure 1. Generation-I and Generation-II Supercapacitors. The NHC device consists of a $Li_4Ti_5O_{12}$ (LTO) negative electrode combined with an activated carbon (AC) positive electrode. This is a hybrid system of a faradaic Li-intercalating LTO electrode and a non-faradaic AC electrode employing anion (typically BF_4^-) adsorption-desorption process. This configuration of the device will produce a larger working voltage and capacitance within the safe voltage range among oxidative and reductive decomposition of electrolytes. The Nanohybrid capacitor (configured as LTO/AC) can produce a higher energy density compared to a conventional (AC/AC) electrochemical capacitor whose energy density is less than 10 Wh L^{-1}.

Figura 1. Supercondensadores de Generación-I y Generación-II.

during charge and discharge [17,18], and 4) safety with little electrolyte decomposition (no SEI (solid electrolyte interface) formation and no gas evolution) [21]. Amatucci *et al.* first introduced the LTO/AC system as a possible battery-capacitor hybrid energy device[24]. However, the conventional LTO electrodes have significant drawbacks such as low power characteristics that stem from an inherently low Li^+ diffusion coefficient (< 10^{-6} cm^2 s^{-1}) and poor electronic conductivity (< 10^{-13} Ω^{-1} cm^{-1}) [21,22].

2. Methods for Preparation and Characterization

In-situ synthesis of nano-LTO precursor and the simultaneous hybridization of two kinds of carbon matrices, carbon nanofiber (CNF) and super-growth carbon nanotube (SGCNT) was carried out using UC treatment [14,15].

Tetrabutyl titanate [$Ti(OC_4H_9)_4$], as a titanium source, was dissolved in isopropyl alcohol. Then, lithium acetate, as a lithium source, was dissolved into a solution of isopropyl alcohol, deionized water, and acetic acid. A mechano-chemical agitation was applied to the carbon-containing mixture for 5 min at 75,000G under the same conditions described elsewhere [14,16]. The precursor composites were obtained after drying the resultant gel at 80 ºC for 17 h *in vacuo*, then calcined for a short duration of 3 min at 900ºC *in vacuo*. The weight ratio of LTO/carbon was controlled by the dosed molar ratios of the Li source and the Ti source.

A CNF, CO-derived carbon nanotube obtained from JEMCO, is a tubular carbon fiber consisting of 10–20 graphene layers that are synthesized through the decomposition of carbon-containing gases via chemical vapor deposition [23]. The diameter and specific surface area (SSA) of the received CNF are 15–20 nm and 400 m^2 g^{-1}, respectively.

A SGCNT, obtained from National Institute of Advanced Industry and Technology (AIST), was used without further purification [27-30]. The SSA measured for the resulting LTO/CNF and LTO/SGCNT composites show typically 99 and 177 m^2 g^{-1}, respectively.

In order to characterize the stoichiometry of the composites, thermal analysis was performed in a temperature range of 25-1000 ºC under air atmosphere (100 ml min^{-1}) using a SII EXSTAR 6000 TG/DTA 6300 thermal analyzer with a heating rate of 5 ºC min^{-1}.

In order to characterize the composites, X-ray diffraction, Raman spectroscopy (Jasco NSR-2100, excited by 514 nm Ar laser) and HRTEM were used in this study. X-ray powder diffraction (Rigaku SmartLab, Cu K*a* radiation λ=1.54056 Å, operating at 45 kV-200 mA) was used to characterize the crystalline structure and crystallite diameter of the LTO in the composites.

HR-TEM (Hitachi H-9500, 300 kV) was used for characterization of the UC-LTO/carbon composites. A sample was ultrasonically dispersed in ethanol for 5 min and dropped onto a microgrid (Okenshoji, Type B Cu150 μm). For a real-time monitoring, the sample was mounted on a special tungsten (W-wire) specimen heating holder,[28] allowing us to precisely control its temperature through the adjustment of the DC current. The temperature was within ± 20ºC precision that was independently calibrated using a pyrometer[31]. The dried LTO/SGCNT (weight ratio=80:20) precursors were subjected to preheating

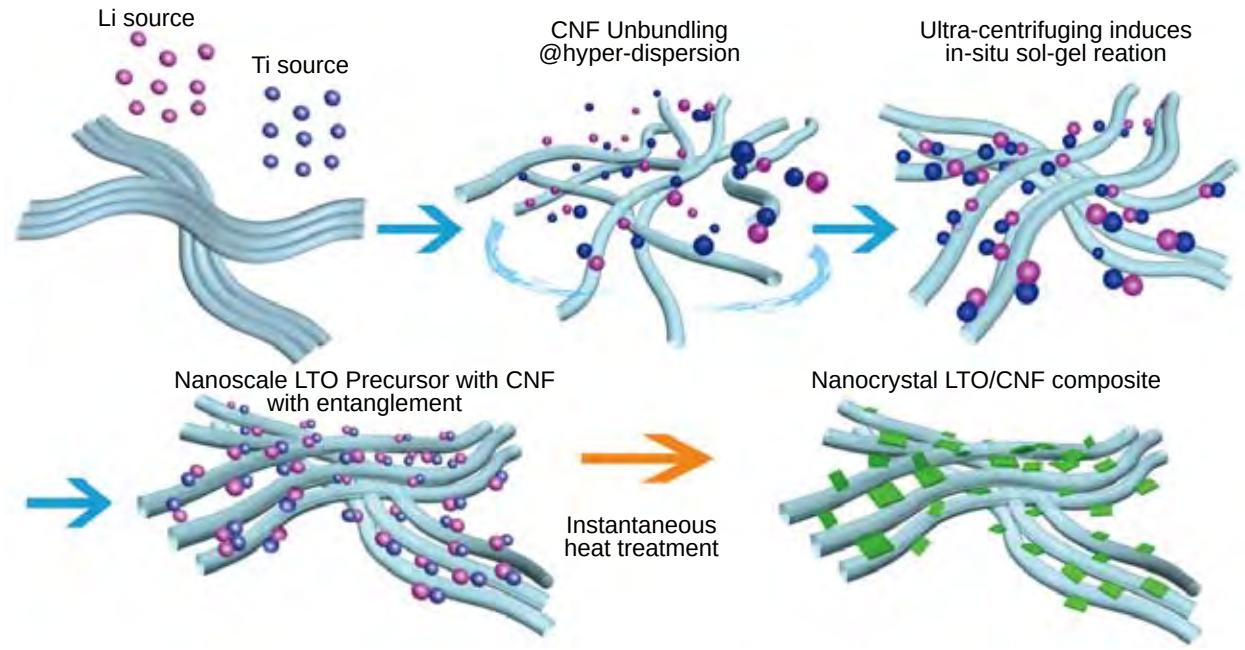

Figure 2. Concept of 'Ultra-Centrifugation (UC).' The UC treatment involves a simple one-step rapid generation scheme yielding a series of optimized 'nano-nano composites,' capable of storing and delivering energy at the highest sustained capacity with remarkable C rates. With this method, we can enhance the rate of many Li-insertion compounds for batteries and utilize them as alternative capacitor electrodes. The UC treatment is a build-up synthetic scheme involving the following 4 steps; **0**: starting materials, *viz.*, carbon matrix (CNF or SGCNT), Ti and Li sources are pre-mixed, **1**: starting ultra-centrifuging which initiates unbundling of the carbon matrix for maximum dispersion in order to obtain the highest probability of contact with reactant species, **2**: sol-gel reaction takes place and produces LTO precursor *in-situ* on carbon, **3**: terminating Ultra-Centrifuging induces rebundling and restructuring of the carbon matrix to form a 'nano-nano composite,' highly dispersed with nanoscale LTO precursors. This process simultaneously produces a mesopore network (that acts as an electrolyte reservoir) of interstices created between the carbon matrixes due to the trapped LTO precursors. **4**: post-heat treatment effectively completes the crystallization process, producing LTO spinel structures without crystal growth (further description in Figure 5).

Figura 2. Concepto de 'Ultracentrifugación (UC).'

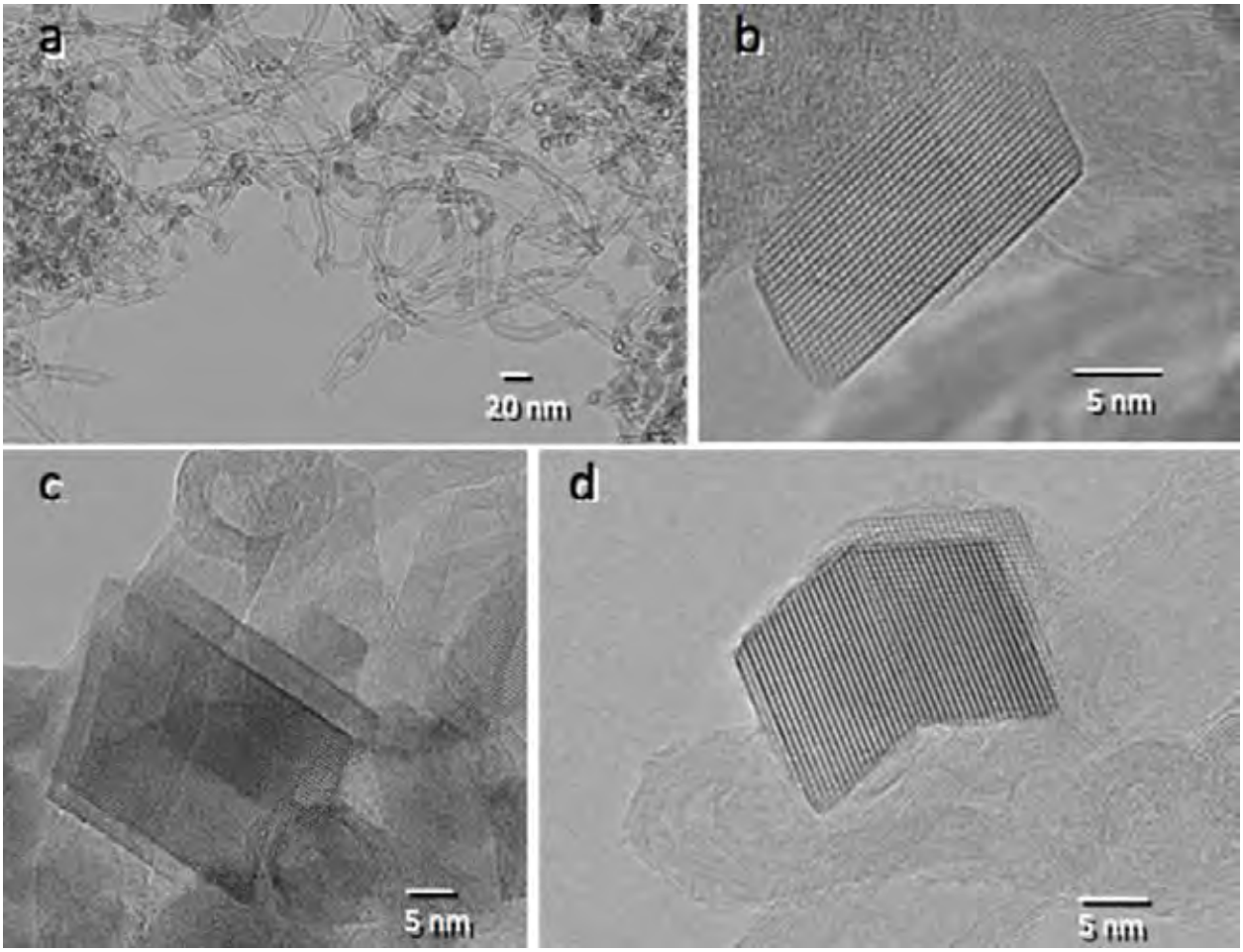

Figure 3. HRTEM images of UC-LTO/CNF nanosheets. a. Overall view of the UC-LTO/CNF (weight ratio of LTO to CNF=70:30). **b.** HRTEM image of UC-LTO/CNF nanosheet. **c.** HRTEM image of UC-LTO nanosheet, clearly demonstrating the 2D-LTO crystals**. d.** HRTEM image of two interconnected LTO twin crystals called a 'nanobook.'

Figura 3. Imágenes de HRTEM de UC-LTO/CNF nanosheets.

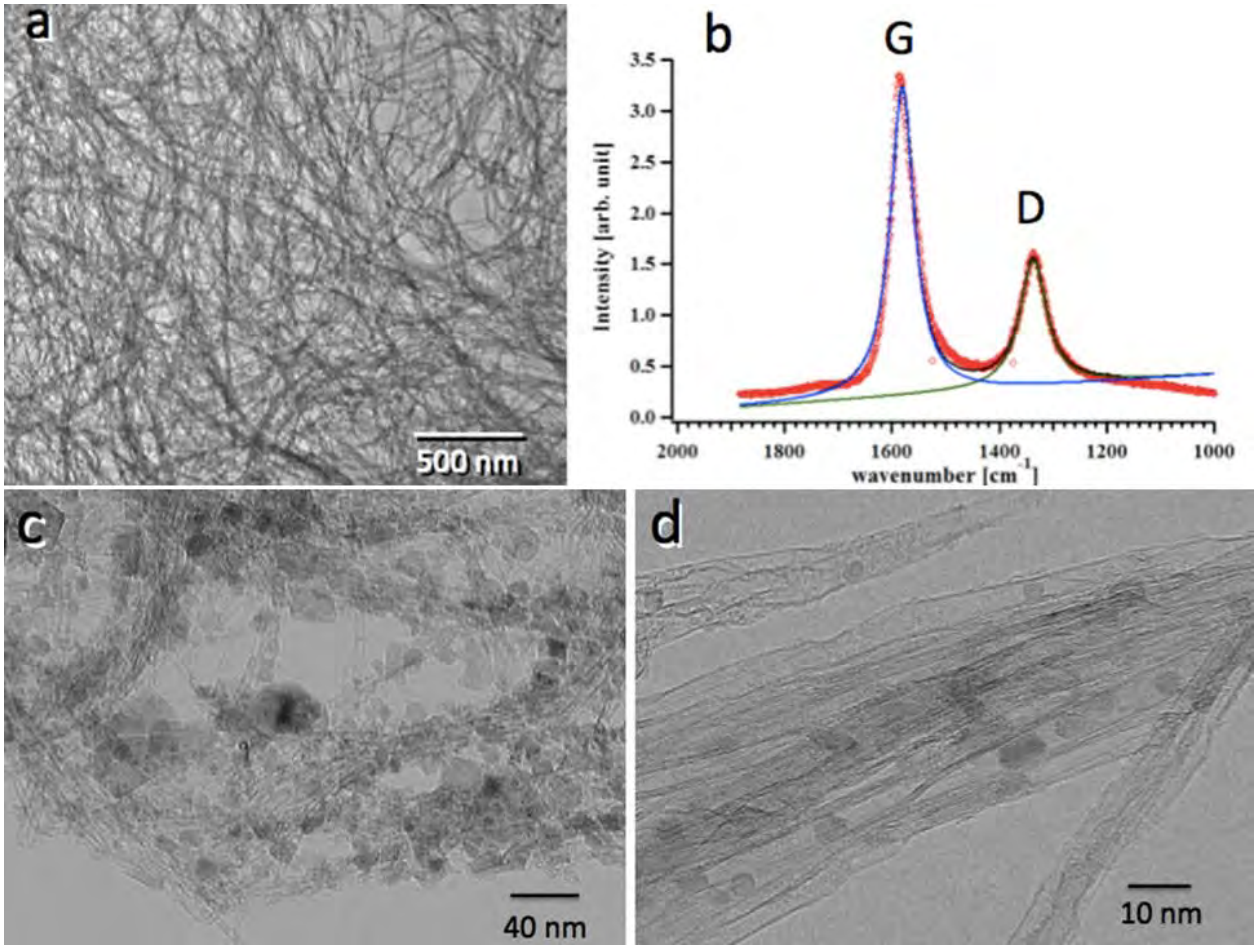

Figure 4. TEM observations of SGCNT and UC-LTO/SGCNT. a. TEM image of a well dispersed and unbundled pristine SGCNT (3-5nm in diameter, specific surface area: 600 m^2 g^{-1}), **b.** Raman spectroscopy of the same SGCNT, showing a fairly high disorder ratio (I_G/I_D =2.4). This is an indication that the SGCNT used here has abundant anchoring sites for LTO to nucleate. **c.** HRTEM image of UC-LTO/SGCNT (the weight ratio of LTO to SGCNT= 80:20), exhibiting highly dispersed LTO particles of about 2 to 20 nm in diameter within the SGCNT network. **d.** HRTEM of UC-LTO/SGCNT (85:15) composite. The high-magnification images confirmed the existence of LTO particles not only within the interstitial spaces of the SGCNT bundles but also inside the single-walled carbon nanotubes in their highly crystalline states**.** By employing SGCNT in our UC treatment, the ratio of LTO to SGCNT can be maximized to 90% while still maintaining the LTO crystals in its small nucleated and single nanosized dimension.

Figura 4. TEM de SGCNT y UC-LTO/SGCNT.

at 400ºC for 30 min and then elevated to 670ºC *in vacuo* in the TEM chamber.

Electrochemical characteristics were evaluated using a half-cell electrode set-up (Li/(UC-LTO/carbon)). The half-cell was assembled with a Li metal electrode and a LTO/carbon electrode, using a 2032 coin-type cell. The electrolyte was a mixture of ethylene carbonate (EC) and dimethyl carbonate (DMC) containing 1.0 M lithium tetrafluoroborate ($LiBF_4$) as an electrolyte salt. The LTO/carbon electrode was prepared by mixing 80% of the composite and 20% of polyvinylidene fluoride (PVDF) in N-Methylpyrrolidone. The mixture was coated on a Cu foil (current collector) and dried at 150 ºC *in vacuo*. The thickness of the LTO/carbon electrode was ca. 20 μm, corresponding to a loading weight of ca. 1 mg. Charge-discharge tests were performed under CC-mode between 1.0 and 3.0 V vs. Li/Li^+ at several current density ranges.

3. Ultra-Centrifugation: A Unique Materials Processing Means for Simultaneous Nanofabrication and NanoHybridization

We used our newly synthesized UC-LTO/carbon composites as the negative electrode in combination with activated carbon as the positive electrode in configuring the 'Nanohybrid capacitor.' As described later, this new capacitor device results in an extremely high-energy performance at the same level of power capability (cycled > 10,000 cycles) that exceeds those of conventional electrochemical capacitors.

4. Dimension Controlled LTO Nanocrystals

The spinel structured LTO has been prepared with two types of hyper dispersed carbons, *viz.*, CNF and SGCNT. As described in our previous papers [14-16], the UC treatment at 75,000G stoichiometrically accelerates the *in situ* sol-gel reaction (hydrolysis followed by polycondensation) and further forms, anchors and grafts the nanoscale LTO precursors onto the carbon matrices. The mechano-chemical sol-gel reaction is followed by a short heat-treatment process *in vacuo*. The instantaneity of the heat-treatment is of utmost importance in achieving high crystallization, inhibiting oxidative decomposition of carbon matrices, and in suppressing agglomeration. In our current research we further optimized this annealing process in order to avoid any oxidative decomposition of carbon. Thermogravimetric (TG) analysis was performed to estimate the weight ratio of LTO to carbon matrices based on the weight of dosed Ti alkoxide before the UC treatment. Annealing at 700˚C under N_2 for 3 minutes was enough to crystallize the LTO/CNF precursors. The XRD peaks for some possible impurities such as TiO_2, Li_2CO_3, and Li_2TiO_3 [29,30] were below the detection limits

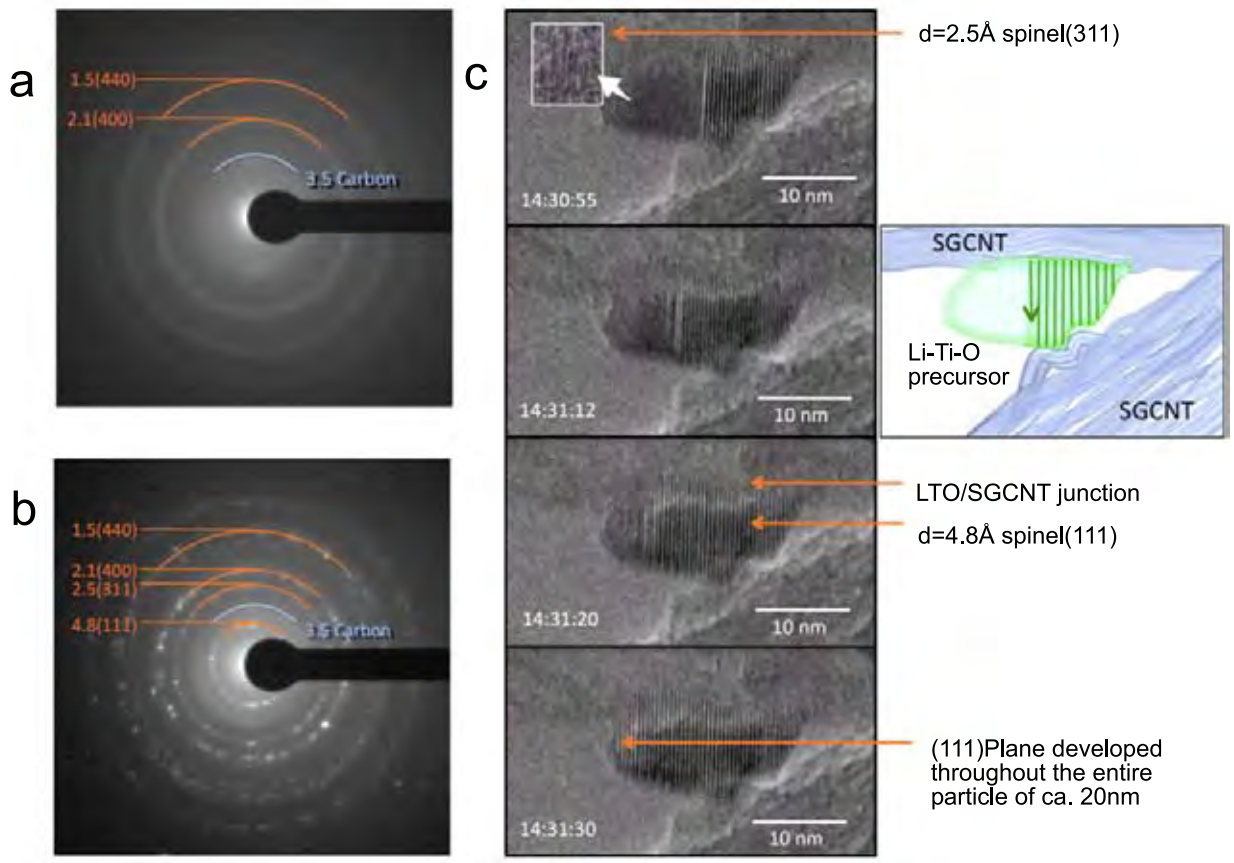

Figure 5. ***in-situ*** **real-time TEM observation during crystallization process of a UC-LTO/SGCNT.** **a.** Electron diffraction patterns of a preheated precursor at 400ºC, showing its pre-crystallized state. **b.** Electron diffraction patterns of the same sample after annealing at 670 ºC. The rings and spots correspond to the d-spacing in Å (lattice plane) for the spinel structures of LTO and carbon. The d spacing of 4.8, 2.5, 2.1, and 1.5 Å correspond to the lattice planes of (111), (311), (400), and (440), respectively. **c.** Magnified views of selected HRTEM images during a consecutive real-time monitoring of the focused UC-treated LTO/SGCNT particle through its process of full crystallization. The development of the vertical (111) fringes can be seen from right to left throughout one particle. Within 45 seconds a single UC-LTO/SGCNT precursor particle was fully crystalized into a spinel LTO.

Figura 5. Observación de TEM *in-situ* a tiempo real durante el proceso de cristalización de UC-LTO/SGCNT.

and the major phase was the spinel-LTO and carbon matrix.

Figure 3a is a HRTEM image of the obtained LTO/CNF, which displays the high dispersion of LTOs among the CNF network. Figures 3b and 3c are magnified high-resolution images that show planar LTO crystals that are grown two-dimensionally on the CNF. These images demonstrate that the 2D LTO-nanosheet is nucleated and developed on the CNF and is firmly attached before the annealing process. As a result of the fast Fourier-transform (FFT) analysis on TEM images, the lattice of the LTO crystals was composed with d spacing of 4.81 Å, which indicates that it is of the spinel (111) plane. By shortening the annealing process, the (111) plane is able to develop both at a rapid pace and in shape with its surrounding carbon matrix. This can be clearly observed in Figure 3c. The direction of the 2D-LTO crystals follows the contour of the CNF matrix to the extent that a very peculiar structure of two interconnected LTO nanosheets in the shape of an open book was formed (Figure 3d). This 'nanobook' of folded LTO/CNF layers suggests that the (111) plane of the LTO nanosheet rapidly changed its direction of growth by about 120 degrees in shape with the contour of the its attached CNF matrix.

5. nc-LTO Composited with SGCNT Interstitials and Inner Tubes

We replaced the CNF with SGCNT, a single-walled carbon nanotube synthesized through a super-growth method [23,26-28] (Figure 4a) as the matrix for the LTO composite. We expected the SGCNT to be a better supporting material due to its high specific surface area, high elemental purity, and high electrical conductivity [27]. The typical I_G/I_D ratio of the used SGCNT specifically for the UC-nanohybridization was 2.4, as obtained through Raman spectroscopy (Figure 4b). This indicates that compared to the normal SGCNT (I_G/I_D is typically 12-14) as reported previously [24] it has a fairly high content of defects acting as optimal anchoring sites for the LTO precursors to nucleate. Figures 4c and 4d show HRTEM images of a high loading LTO/SGCNT (80% LTO) in which highly dispersed LTO particles of about 2 to 20 nm in diameter can be clearly observed in the SGCNT network. In addition, the high-magnification images confirmed the existence of the LTO particles not only within the interstitial spaces of the SGCNT bundles but also inside the tubes in their highly crystalline states (Figure 4d). By employing SGCNT in our UC treatment, the ratio of LTO to SGCNT was increased to 90% while still maintaining the LTO nanocrystals in single digit size. This allows for further enhancement in both energy and power capabilities.

6. Real-Time and In-situ HRTEM Observation of Crystallization Process

Real-time monitoring of the LTO annealing process was conducted through the use of *in-situ* HRTEM (Figure 5). A sequence of high-resolution electron micrographs shows the *in-situ* crystallization of UC-LTO/SGCNT at 670ºC. What becomes immediately

apparent is the fact that despite crystallization, no growth in size of the LTO was observed. This can be partially explained due to its confinement within the cavity-crated entanglement of the carbon nest as well as other optimal accommodations during the annealing process.

Electron diffraction (ED) analysis was performed during pre-annealing at 400 °C (Figure 5a) and post-annealing at 670°C (Figure 5b) to confirm the formation of the LTO crystal structures and the unchanged presence of the SGCNT. The post-annealing ED pattern seen in Figure 5b clearly indicates the presence of face-centered cubic spinel structures with a $Fd\bar{3}m$ space group [17,18].

To further examine the crystallization process, we recorded in real-time the partial crystallization of a LTO particle. Figure 5c shows magnified views of selected HRTEM images during the monitoring period, focusing on one LTO precursor particle for 45 seconds through its process into a fully crystallized spinel structure. Recorded after the formation of roughly half the crystal, the crystallization process proceeded very rapidly with the immediate formation of a fully crystallized particle of 20 nm in diameter within a mere 45 seconds. Approximately every 4.8 Å we observed a new fringe, suggesting the formation of a spinel (111) plane, characterized by its d spacing of 4.8 Å. In its process of development, we also observed traces of (311) planes with smaller d spacing of 2.5 Å immediately prior to the formation of the (111) planes.

7. Ultrafast Supercapacitor Performances

Figure 6a shows the charge-discharge curves of the half-cell Li/UC-LTO/SGCNT between 10C and 1200C. The dominant plateau was observed at 1.55 V (*vs.* Li/Li$^+$), indicating the Li$^+$ intercalation-deintercalation of a spinel LTO [17,19]. A highly loaded LTO composite (with the LTO/SGCNT ratio of 80:20) showed a specific capacity of 130 mAh g^{-1} (per composite) at 10C (1C=175 mAh g^{-1}). This value is *ca.* 93 % of the theoretical capacity of LTO. Remarkably, the composite showed 107 mAh g^{-1} at 300C and 78 mAh g^{-1} (60 % retention) even at 1200C. In other words, the high retention of the LTO specific capacity is attained despite such high C rates in the higher ranges above 300C.

Figure 6b further demonstrates that the retention of specific capacity of UC-LTO/SGCNT at high C rates is even higher than that of UC-LTO/CNF. Such a remarkably high rate capability of the LTO composite is due to the unusually small nanocrystalline LTO particles that increase electrochemical utilization and the mesopore network of the CNF that allows an entanglement effect of the nano-LTO and nano-SGCNT. These two aspects enable hyper diffusivity

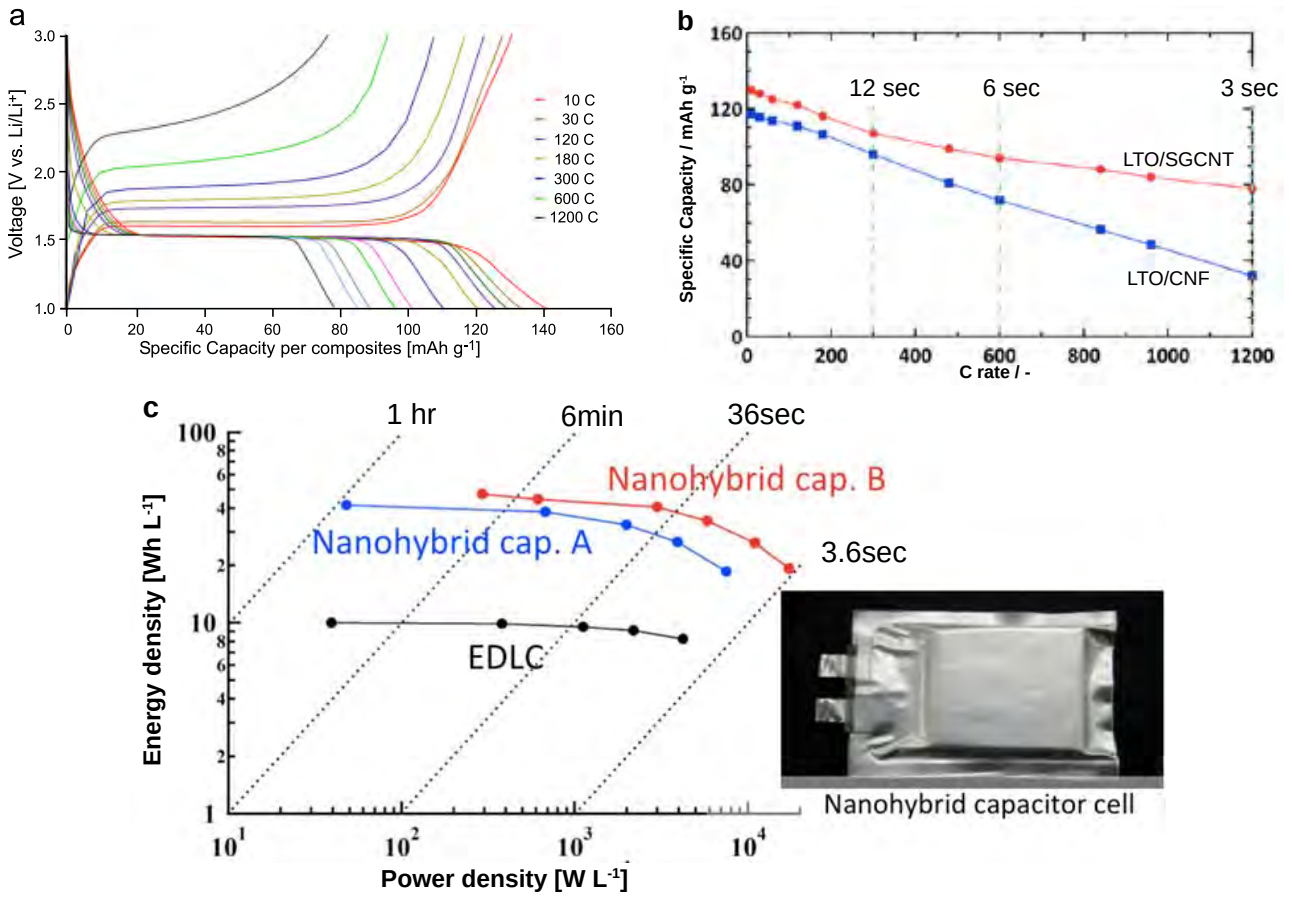

Figure 6. Supercapacitor performances of Nanohybrid capacitor using UC-LTO/CNF and UC-LTO/SGCNT. a. Charge-discharge profiles for a LTO/SGCNT electrode, exhibiting unusually high charge retention at C rates in the higher ranges of 300C to 1200C. Such a remarkably high response of the LTO composite is due to the nano-sizing of the LTO particles and the mesopore network of the carbon nano-fibers that allows an entanglement effect of the nano-LTO and nano-SGCNT. This enables hyper diffusivity and accessibility of the electrolyte, leading to an increase in electrical conductivity. **b.** Delivered specific capacity as a function of C rate for half-cell capacitors utilizing UC-LTO/CNF and UC-LTO/SGCNT. This demonstrates that the retention of specific capacity of UC-LTO/SGCNT at high C rates is even higher than that of UC-LTO/CNF. **c.** Ragone plots for two full cell capacitors; 'Nanohybrid capacitor A'[UC-LTO/CNF (70:30)]/AC] and 'Nanohybrid capacitor B'[UC-LTO/SGCNT (80:20) /SGCNT]. A full cell for a normal EDLC (AC/1M $TEMABF_4$/PC/AC) employs as a reference and measured in the same conditions above.

Figura 6. Funcionamiento del condensador nanohíbrido que usa LTO/CNF y UC-LTO/SGCNT.

and accessibility of the electrolyte, thus enhancing ionic conductivity.

Such LTO composites (both UC-LTO/CNF and UC-LTO/SGCNT) were utilized in combination with two kinds of positive electrodes, viz., activated carbon and SGCNT in creating full laminate cells of 'Nanohybrid capacitors.' The Nanohybrid capacitor A and B comprise of [UC-LTO/CNF (70:30)]/1M $LiBF_4$/EC+DMC/AC and [UC-LTO/SGCNT (80:20)]/1M $LiBF_4$/EC+DMC/SGCNT, respectively are tested for their energy-power performances in the same conditions as a reference EDLC (AC/1M $LiBF_4$/PC/AC) cell. Figure 6c shows Ragone plots for the Nanohybrid capacitor cells A, B and EDLC cell obtained from the charge-discharge curves (10-300C). In a low power density range of 0.1-1 kW L^{-1}, the nanohybrid capacitors show energy densities as high as 28-30 Wh L^{-1}, which is a value comparable to that of Li-ion capacitors [6,10]. Even at a high power density of 6 kW L^{-1}, the energy densities of the nanohybrid capacitors remain at 15 Wh L^{-1}, which is double that of conventional electrochemical capacitors. The result reveals that Nanohybrid capacitor A can provide 3 times higher energy than the existing alternatives in both ranges of low power density (0.1-1 kW L^{-1}) and Nanohybrid capacitor B showed 4.5 times higher energy density than the conventional EDLC cell even at high power density of 1-6 kW L^{-1}. It should be noted however that the utilization and a real application of the SGCNT in a large-scale practical supercapacitor device should await its further cost down by nearly a factor of 1/10. However, the Nanohybrid capacitor configuration as a new generation supercapacitor system can be one of the realizable alternatives because the SGCNT is only used in some portion, e.g., 20% within the whole composite electrode materials (LTO/SGCNT=80:20 as shown in Figure 6). This suggests a strong strategy to save the cost of capacitor devices by reducing the dosage of the expensive SGCNT material.

8. Outlook

Electrochemical capacitors utilize activated carbons for both positive and negative electrodes that show non-faradaic, double-layer charging-discharging mechanism in symmetric configuration. Thus the electrochemical capacitors are efficient energy storage devices that exhibit long lifespans and extremely rapid charge-discharge characteristics compared with batteries. Today, the capacitor technology is regarded as a promising means and has an additional advantage with increasing effectiveness when combined with solar and wind regenerative energy sources. In recent years, nano-composite battery materials have been vigorously researched in hopes to improve their energy density. Hybridizing battery and capacitor materials overcomes the energy density limitation of existing generation-I capacitors without much sacrificing the cycling performances. Normal battery-capacitor hybrids employ high-energy & sluggish redox electrode and low-energy & fast double-layer electrodes, possibly producing a larger working voltage and higher over-all capacitance. In order to smoothly operate such asymmetric systems, however, the rates of the two different electrodes must be highly balanced. Especially, the redox rates of the battery electrodes must be substantially increased to the levels of double-layer process. In this report, we attempt to identify the essential issues for the realizable hybrids and suggest ways to overcome the rate enhancement by exemplifying ultrafast performance of the $Li_4Ti_5O_{12}$ nanocrystal prepared via a unique *in-situ* material processing technology under ultra-centrifuging.

9. Acknowledgments

The authors are indebted to K. Hata, AIST Japan and S. Iijima (Meijo University, Japan) for supplying SGCNT through NEDO project, Carbon Nanotube Capacitor Project (2006-2011). K.N. is grateful to Y. Gogotsi and B. Dyatkin (Drexel University, U.S.A.) and P. Simon (Paul Sabatier University, France) for valuable discussions. Special thanks to S. Ishimoto (Nippon Chemi-con Corp.) for fabricating test capacitor cells for obtaining supercapacitor performances (Ragone plots).

10. References

[1] Simon P, Gogotsi Y. Materials for electrochemical capacitors. Nature Mater. 2008; 7: 845.

[2] Chmiola J, Largeot C, Taberna P-L, Simon P, Gogotsi Y. Monolithic Carbide-Derived Carbon Films for Micro-Supercapacitors. Science 2010; 328: 480-483.

[3] Gao W, Singh N, Song L, Liu Z, Reddy ALM, Ci L, Vajtai R, Zhang Q, Wei B, Ajayan P M. Direct laser writing of micro-supercapacitors on hydrated graphite oxide films. Nature Nanotechnol. 2011; 6:496-500.

[4] Pech D, Brunet M, Durou H, Huang P, Mochalin V, Gogotsi Y, Taberna P-L, Simon P. Ultrahigh-power micrometre-sized supercapacitors based on onion-like carbon. Nature Nanotechnol. 2010; 5:651-654.

[5] Lee SW, Yabuuchi N, Gallant BM, Chen S, Kim B-S, Hammond PT, Shao-Horn Y. High-power lithium batteries from functionalized carbon-nanotube electrodes. Nature Nanotechnol. 2010; 5:531-537.

[6] Burke A. Ultracapacitors: why, how, and where is the technology. J. Power Sources 2000; 91:37.

[7] Pandolfo AG, Hollenkamp AF. Carbon properties and their role in supercapacitors. J. Power Sources 2006; 157: 11.

[8] Kötz R, Carlen M. Principles and applications of electrochemical capacitors. Electrochim. Acta 2000; 45:2483-2498.

[9] Plitz I, Dupasquier A, Badway F, Gural J, Pereira N, Gmitte, A, Amatucci GG. The design of alternative nonaqueous high power chemistries. Appl. Phys. A 2006; 82:615-626.

[10] Naoi K, Simon P. New Materials and New Configurations for Advanced Electrochemical Capacitors. Interface 2008; 17:34-37.

[11] Lang X, Hirata A, Fujita T, Chen M. Nanoporous metal-oxide hybrid electrodes for electrochemical supercapacitors. Nature Nanotechnol. 2011; 6:232-236.

[12] Wang Q, Wen Z, Li J. Carbon nanotube/TiO_2 nanotube hybrid supercapacitors, J. Nanosci. Nanotech. 2007; 7:3328-3331.

[13] Zhang W-D, Xu B, Jiang LC. Functional hybrid materials based on carbon nanotubes and metal

oxides, J. Mater. Chem. 2010; 20:6383-6391.

[14] Naoi K, Ishimoto S, Ogihara N, Nakagawa Y, Hatta S. Encapsulation of Nanodot Ruthenium Oxide into KB for Electrochemical Capacitors. J. Electrochem. Soc. 2009; 156: A52-59.

[15] Naoi K, Ishimoto S, Isobe Y, Aoyagi S. High-rate nano-crystalline $Li_4Ti_5O_{12}$ attached on carbon nano-fibers for hybrid supercapacitors. J. Power Sources 2010; 195:6250-6254.

[16] Naoi K. Nanohybrid Capacitor: The Next Generation Electrochemical Capacitors. Fuel Cells 2010; 10:825-833.

[17] Ohzuku T, Ueda A, Yamamoto N. Zero-Strain Insertion Material of $Li[Li_{1/3}Ti_{5/3}]O_4$ for Rechargeable Lithium Cells. J. Electrochem. Soc. 1995; 142:1431-1435.

[18] Thackeray MM. Structural Considerations of Layered and Spinel Lithiated Oxides for Lithium Ion Batteries. J. Electrochem. Soc. 1995; 142: 2558-2563.

[19] Jansen AN, Kahaian AJ, Kepler KD, Nelson PA, Amine K, Dees DW, Vissers DR. Development of a high-power lithium-ion battery. J. Power Sources 1999; 81-82:902-905.

[20] Scharner S, Weppner W, Schmind-Beurmann P. Evidence of Two-Phase Formation upon Lithium Insertion into $Li_{1.33}Ti_{1.67}O_4$ Spinel J. Electrochem. Soc. 1999; 146: 857-861.

[21] Shu, J. Study of the Interface Between $Li_4Ti_5O_{12}$ Electrodes and Standard Electrolyte Solutions in 0.0-5.0 V. Electrochem. and Solid-State Letters 2008; 11:A238-240.

[22] Amatucci, G. G., Badway, F., Pasquier, A. D. and Zheng, T. An Asymmetric Hybrid Nonaqueous Energy Storage Cell. J. Electrochem. Soc. 2001; 148:A930-939.

[23] Zou JH, Sui ZJ, Li P, Chen D, Dai YC, Yuan WK. Structural characterization of carbon nanofibers formed from different carbon-containing gasses. Carbon 2006; 44: 3255-3262.

[24] Hata K, Futaba DN, Mizuno K, Namai T, Yumura M, Iijima S. Water-Assisted Highly Efficient Synthesis of Impurity-Free Single-Walled Carbon Nanotubes. Science 2004; 306: 1362-1367.

[25] Yuge R, Miyawaki J, Ichihashi T, Kuroshima S, Yoshitake T, Ohkawa T, Aoki Y, Iijima S, Yudasaka M. Highly Efficient Field Emission from Carbon Nanotube−Nanohorn Hybrids Prepared by Chemical Vapor Deposition. ACS Nano 2010; 4:7337-7343.

[26] Hiraoka T, Izadi-Najafabadi A, Yamada T, Futaba DN, Yasuda S, Tanaike O, Hatori H, Yumura M, Iijima S, Hata K. Compact and Light Supercapacitor Electrodes from a Surface-Only Solid by Opened Carbon Nanotubes with 2 200 m^2 g^{-1} Surface Area. Adv. Func. Mater. 2010; 20:422-428.

[27] Izadi-Najafabadi A, Futaba DN, Iijima S, Hata K. Ion Diffusion and Electrochemical Capacitance in Aligned and Packed Single-Walled Carbon Nanotubes. J. Am. Chem. Soc. 2010; 132:18017-18019.

[28] Kamino T, Saka H. A newly developed high-resolution hot stage and its application to materials characterization. Microsc. Microanal. Microstruct. 1993; 4:127-135.

[29] Takai S, Kamata M, Fujiine S, Yoneda K, Kanda K, Esaka T. Diffusion coefficient measurement of lithium ion in sintered $Li_{1.33}Ti_{1.67}O_4$ by means of neutron radiography. Solid State Ionics 1999; 123: 165-172.

[30] Chen CH, Vaughey JT, Jansen AN, Dees DW, Kahaian AJ, Goacher T, Thackeray MM. Studies of Mg-Substituted $Li_{4-x}MgxTi_5O_{12}$ Spinel Electrodes ($0 \leq x \leq 1$) for Lithium Batteries. J. Electrochem. Soc. 2001; 148: A102-104.